Homo-epitaxial diamond film growth on ion implanted diamond substrates.

PAUL S. WEISER, STEVEN PRAWER, KERRY W. NUGENT, ANDREW A. BETTIOL,
LOUIE I. KOSTIDIS AND DAVID N. JAMIESON.
School of Physics, MARC, The University of Melbourne, Parkville, Victoria 3052, Australia.

INTRODUCTION

The nucleation of CVD diamond is a complicated process, governed by many interrelated parameters. In the present work we attempt to elucidate the effect of strain on the growth of a homo-epitaxial CVD diamond. We have employed laterally confined high dose (MeV) Helium ion implantation to produce surface swelling of the substrate. The strain is enhanced by the lateral confinement of the implanted region to squares of 100×100 μm^2. After ion implantation, micro-Raman spectroscopy was employed to map the surface strain. The substrates were then inserted into a CVD reactor and a CVD diamond film was grown upon them. Since the strained regions were laterally confined, it was then possible to monitor the effect of strain on diamond nucleation. The substrates were also analysed using Rutherford Backscattering Spectroscopy (RBS), Proton induced X-ray Emission (PIXE) and Ion Beam induced Luminescence (IBIL).

EXPERIMENT

The diamond substrates were 3×3 mm^2 (100) faces of natural diamonds from Argyle diamond mines. The substrates were inserted into the Micro-Analytical Research Centre's (MARC) Nuclear Microprobe and evacuated to a base pressure better than 5×10^{-6} Torr. The diamond substrates were implanted with 2 MeV He ions in the random orientation over an area of 100×100 μm^2 with a dose of 5.0×10^{16} ions/cm^2. (The ion range, Rp, and straggling, ΔRp, as predicted by TRIM90 [1], for randomly aligned 2 MeV He ions into diamond are 3.46 μm and 0.05 μm respectively.) Further information regarding the implantation technique can be found in ref. [2]. The implanted squares were analysed using a surface profilometer and micro-Raman spectroscopy.

The Raman measurements were taken using a Dilor XY confocal micro-Raman spectrometer employing the 514 nm line from an Ar ion laser with a $\times 100$ objective and a confocal aperture of 50 μm. The confocal optical arrangement is such that, even though diamond is transparent to the 514 nm light used in the Raman measurement, the sampling volume is restricted to a cylinder of diameter 1 μm and depth 2 μm. A depth scan is performed by varying the position of the focus of the laser using a piezoelectric driven objective. A shift in the Raman peak to higher energy is indicative of compressive strain, while a shift to lower energy is indicative of tensile strain [3].

After Raman analysis the samples were inserted into a hot-filament CVD deposition system. The CVD deposition conditions were: pressure 30 Torr; total flow 100 sccm; 1% CH_4; deposition temperature 1000°C and deposition time 4 hours. The samples were then re-analysed using surface profilometry and micro-Raman Spectroscopy.

RBS, PIXE and IBIL spectra were then collected using the Nuclear Micro-probe. A 20μm beam spot was employed. IBIL spectroscopy enables a clear distinction between high quality natural diamond (blue peak) and CVD diamond films (green peak) [4]. By varying the analysing beam energy we obtain information from varying depths within the substrate. Firstly, 3 MeV H^+ (Rp + ΔRp = 47.6 + 0.76 μm) was chosen to investigate the natural diamond substrate beneath the CVD diamond film. Secondly, a 1.4 MeV H^+ beam (Rp + ΔRp = 13.6 + 0.25 μm) was employed, enabling a more selective analysis of the CVD diamond film ($\sim$5 μm) and the underlying natural diamond. Thirdly, a 2 MeV H_2^+ (molecular Hydrogen) beam (Rp + ΔRp = 7.98 + 0.16 μm) was employed to investigate the CVD diamond film. (The molecular Hydrogen splits up on impact with the sample producing 1 MeV H^+ ions.)

RESULTS AND DISCUSSION

Figure 1 shows the shift in the Raman diamond line position in steps of 5 μm across a 5.0×10^{16} ions/cm^2 2 MeV random He implant. The Raman diamond line position from the surface of the implant is shifted to lower energy by on average 5.4 cm^{-1} (FWHM, 12 cm^{-1}) from its unstrained value of 1331.3 cm^{-1} (FWHM, 3.2 cm^{-1}). The diamond line is broadened indicating that the strain in the cap is caused by defects in the cap, rather than by the end of range damage [5]. Recently, K.W. Nugent et al [6] have identified two new Raman peaks at 1497 and 1630 cm^{-1} associated with damage centres in diamond. Figure 1 plots the ratio of the 1497 cm^{-1} defect peak to that of the 1332 cm^{-1} diamond line across the surface of the implant. The presence of the 1497 cm^{-1} peak confirms that the strain is induced by defects in the cap layer itself.
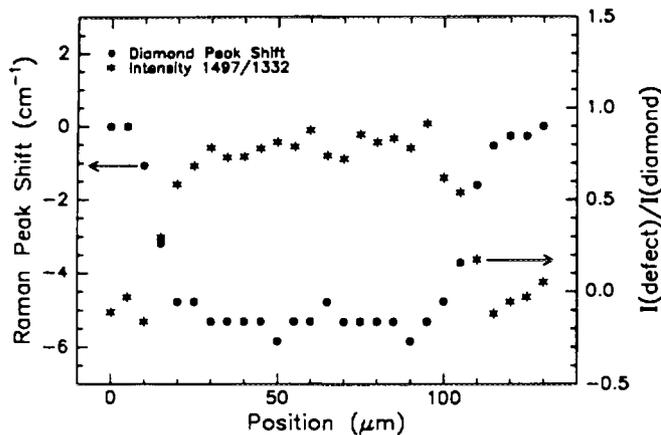
Figure 1. The Raman diamond peak position as a function of position across the implant. Also shown is the ratio of the intensity of the 1497 cm^{-1} peak to that of the 1332 cm^{-1} peak.
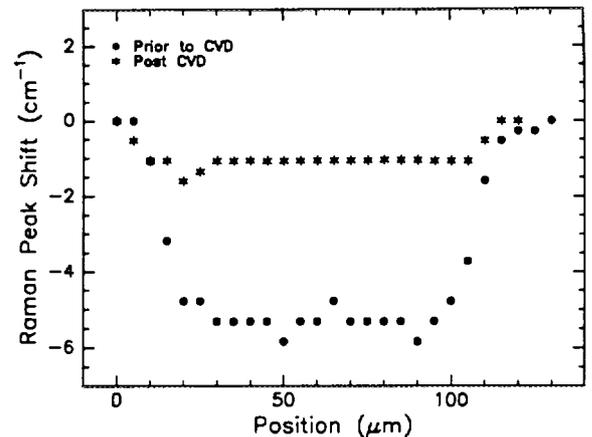
Figure 2. The Raman diamond peak position as a function of position across the implant post and prior to 4 hours of CVD diamond deposition.

After CVD, optical microscopy showed that a film has grown over the entire surface of the diamond substrate. Surface profilometry shows that the rate of diamond film growth on the implanted and unimplanted diamond substrate is the same. The deposited film was established as being homo-epitaxial, with respect to the substrate, by comparing polarised Raman azimuthal scans of the surface of the deposited diamond film and of the underlying diamond substrate at a depth greater than 8 µm below the surface [see ref. 7 for details of this technique].

After CVD, the Raman spectra were once again performed across the surface of the implant. The shift in the diamond line across the implant is plotted in figure 2 (the shift across the implant prior to the CVD is also shown). The diamond line of the implant is still shifted to lower energy by, on average, 1.1 cm^{-1}. There is no evidence of the 1497 and 1630 cm^{-1} damage peaks. In addition, the FWHM of the diamond line is 3.7 cm^{-1}. The absence of the damage peaks and the shift in the diamond line back towards its unstrained value could be due to either (i) the growth of an epitaxial film or alternatively (ii) to the annealing of the ion-induced damage which has been observed at these temperatures [6]. For this reason a depth scan of the Raman spectra in the implanted region was performed. Figure 3 shows the ratio of the intensity of the 1497 cm^{-1} damage peak to the diamond line on the implant as a function of depth from the surface. The 1497 cm^{-1} peak is absent for the first 5 µm of the depth profile, but then its value rises and reaches a steady value about 10 µm below the surface. There is no change in the diamond line position or FWHM throughout the depth profile. These results are consistent with an incompletely annealed implanted layer lying underneath a ~5 µm thick homo-epitaxial diamond film.

The Raman spectra of the film grown on the unimplanted diamond shows a large fluorescent background, which is not observed from the film grown on the implanted region. The inset to figure 3 is a depth profile performed on the film grown on the unimplanted diamond, showing the ratio of the fluorescent background intensity to that of the diamond. The large fluorescent background is present for the first ~5 µm, consistent with the thickness of the
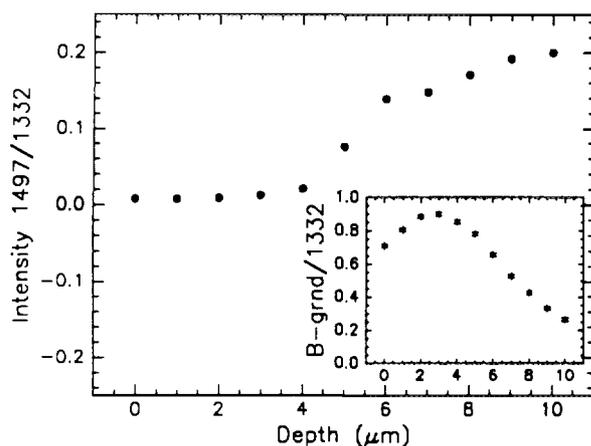

Figure 3. The ratio of the intensity of the 1497 cm^{-1} damage peak to that of the diamond line (on the implant) as a function of depth after CVD deposition. The inset shows the ratio of the fluorescent background to the diamond peak intensity into the diamond grown on the unimplanted diamond.
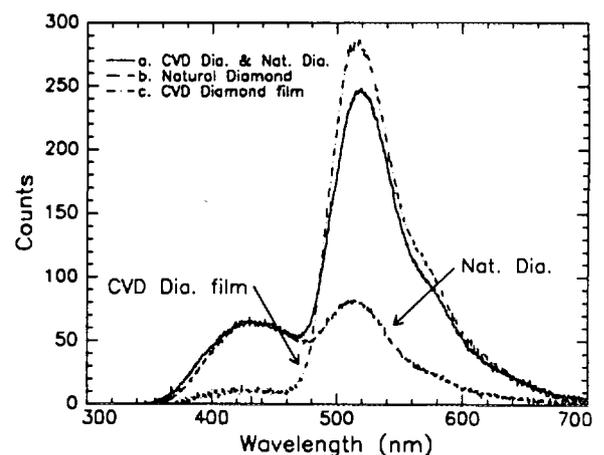
Figure 4. 3 MeV H$^+$ IBIL spectra from (a) the CVD diamond film and the underlying natural diamond substrate, (b) the uncoated natural diamond substrate and (c) the 2 MeV H$_2^+$ IBIL spectra of the CVD diamond film.

78

diamond film grown on the diamond substrate. In general, the fluorescent yield increases with defect density; however caution must be exercised since a high defect concentration can also act to quench fluorescence. Therefore all we can state at present is that the defect structure of the homo-epitaxial film grown on the implanted diamond is different to that grown on the unimplanted diamond. The presence of residual strain in the homo-epitaxial film grown on the implanted region as compared to the strain free film grown on the unimplanted diamond supports this assertion.

Figure 4 shows the 3 MeV H^+ IBIL spectra of (a) the CVD diamond film and the underlying natural diamond substrate and (b) the uncoated natural diamond substrate. Figure 4(c) shows the 2 MeV H_2^+ IBIL spectra of the CVD diamond film (figure 4(c) has been scaled to fit on the same graph as the 3 MeV H^+ spectra). The IBIL results show that while the natural diamond substrate is an even mix of blue (425 nm, 2.9 eV) and green (515 nm, 2.4 eV) the spectra from the CVD diamond film is entirely green. (Note that only the ratio of the green to blue peak heights can be compared between the different beam energies.) The light emitted from the CVD film (2 MeV H_2^+) above the implanted regions of the diamond substrate was too low in intensity to be detected by our Ocean Optics CCD array spectrometer. This is consistent with the very low luminescent yield observed in the Raman spectra. Visually the light emitted from the CVD diamond above the implant appears more blue (similar to that of the uncoated, unimplanted natural diamond) when compared to the light from the CVD diamond grown on the unimplanted portion of the diamond. Hence, since the homo-epitaxial diamond film is of low luminescent yield, it may indeed be transparent and the luminescence observed may be coming solely from the underlying natural diamond substrate.

The PIXE spectra obtained, using 1.4 MeV H^+, is shown in the inset to figure 5. This spectra shows that the only impurity within the first 13.6 μm of the CVD diamond film/natural diamond interface is some W. The RBS spectra, obtained simultaneously from the same region of the sample, shows the expected C edge and surprisingly, a peak situated at 730 keV. Interestingly, there is no W present at the surface. When a RBS simulation is performed, taking into account the non-Rutherford C cross section at this energy, it is found that the peak at 730 keV is attributable to a layer of CVD diamond film containing 0.5% W buried 6.25 μm below the surface of the CVD diamond. The thickness of this W containing layer is 5000 Å. The source of the W is undoubtedly from the W filament used in the CVD deposition process, with W being deposited over the entire surface of the diamond and covering both implanted and unimplanted portions of the substrate. The Raman fluorescence data, showing no fluorescence from the CVD film above the implanted natural diamond and fluorescence from the CVD above the unimplanted natural diamond, suggests that the W impurity is not responsible for the observed fluorescence
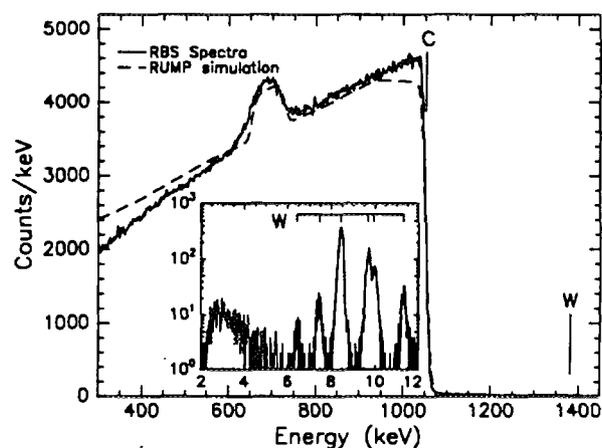

Figure 5. 1.4 MeV H^+ RBS spectra of the CVD coated natural diamond substrate and RUMP simulation showing a 5000 Å layer containing 0.5 % W 6.25 μm below the surface. The inset shows the PIXE spectra obtained.

CONCLUSION

In order to investigate the effect of strain on the nucleation density of CVD deposited diamond we have employed high dose Helium ion implantation into diamond substrates, to produce surface swelling of the substrate. Raman spectroscopy revealed that the surfaces of the implanted regions are under tensile strain (up to 2.7 GPa). The growth rate of homo-epitaxial diamond is the same on the implanted and unimplanted regions of the diamond substrate. However, the CVD film grown on the implanted region shows slight residual tensile strain, but a reduced fluorescent yield as compared with the film grown on the unimplanted diamond substrate. The results show that defects and strain in the diamond substrate can influence the properties of homo-epitaxial diamond films.

REFERENCES

1. TRIM90 - J.F. Ziegler and J.P. Biersack, *The Stopping and Ranges of Ions in Solids*, (Pergamon, New York, 1988).
2. S.P. Dooley and D.N. Jamieson, Nuclear Instruments and Methods in Physics Research B66, p369, (1992).
3. D.S. Knight and W.B. White, J. Mater. Res., 4, p385, 1989.
4. A.A. Bettiol, D.N. Jamieson, S Prawer and M.G. Allen, Nucl. Inst. and Meth. in Phys. Res. B 85, p775, 1994.
5. D.N. Jamieson, S. Prawer, K.W. Nugent and S.P. Dooley, *In Press*, Nucl. Inst. and Meth. in Phys. Res. B, 1995.
6. K.W. Nugent, S.P. Dooley, S. Prawer and D.N. Jamieson, In Preparation.
7. P. John, D.K. Milne, P.G. Roberts, M.G. Jubber, M. Liehr and J.I.B. Wilson, J. Mater. Res., 9(12), p3083, 1994